PERGAMON

Available at
www.ElsevierComputerScience.com
POWERED BY SCIENCE DIRECT

Pattern Recognition 37 (2004) 393–408

PATTERN RECOGNITION
THE JOURNAL OF THE PATTERN RECOGNITION SOCIETY

www.elsevier.com/locate/patcog

A new algorithm for ball recognition using circle Hough transform and neural classifier

T. D'Orazio[a,*], C. Guaragnella[b], M. Leo[a], A. Distante[a]

[a]ISSIA–CNR, Institute of Intelligent Systems for Automation, National Research Council, 166/5, Amendola, Bari 70126, Italy
[b]DEE–Electrics and Electronics Dept.–Politecnico di Bari, 4, E. Orabona, Bari 70125, Italy

Received 22 November 2002; accepted 19 June 2003

Abstract

A large number of methods for circle detection have been studied in the last years for several image processing applications. The context application considered in this work is the soccer game. In the sequences of soccer images it is very important to identify the ball in order to verify the goal event. This domain is a challenging one as a great number of problems have to be faced, such as occlusions, shadows, objects similar to the ball, real-time processing and so on. In this work a visual framework trying to solve the above-stated problems, mainly considering real-time computational aspects, has been developed. The ball detection algorithm has to be very simple in terms of time processing and also has to be efficient in terms of false positive rate. Our framework consists of two sequential steps for solving the ball recognition problem: the first step uses a modified version of the directional circle Hough transform to detect the region of the image that is the best candidate to contain the ball; in the second step a neural classifier is applied on the selected region to confirm if the ball has been properly detected or a false positive has been found. Some tricks like background subtraction and ball tracking have been applied in order to maintain the search of the ball only in limited areas of the image. Different light conditions have been considered as they introduce strong modifications on the appearance of the ball in the image: when the image sequences are taken with natural light, as the light source is strictly directional, the ball, due to self-shades, appears as a spherical cap; this case has been taken in account and the search of the ball has been modified in order to manage this situation. A large number of experiments have been carried out showing that the proposed method obtains a high detection score.

Keywords: Circle detection; Self shadow effects; Neural classifier; Feature detection; Real-time image processing; Object recognition

1. Introduction

Automatic ball recognition in soccer image sequences is a fundamental task: a number of doubtful cases occur during the game, as for example, detecting the outside event or the goal event. An automatic method that detects in each image the ball position is the first and the most important step to build a (non-invasive) vision-based decision support tool for the referee committee during the game.

The soccer domain is challenging as a great number of problems have to be managed, comprising, but not limited to, occlusions, shadowing, misdetection (wrong detection of objects similar to the ball), real-time processing. The ball detection method has to be very simple, fast and effective as a great number of images per second must be processed. Anyway, if some a priori information is available, it can be explicitly used to reduce interpretation and computational time cost.

This kind of problem can be faced considering two different detection systems: geometric approaches can be applied to match a model of the object of interest to different parts of the image in order to find the best fit; example based

* Corresponding author. Tel.: +39-080-548-1969; fax: +39-080-548-311.
E-mail address: dorazio@ba.issia.cnr.it (T. D'Orazio).

0031-3203/$30.00 © 2003 Pattern Recognition Society. Published by Elsevier Ltd. All rights reserved.
doi:10.1016/S0031-3203(03)00228-0

techniques can be applied to learn the salient features of a class of objects from sets of positive and negative examples.

The detection of circles in digital images by using geometric approaches has been largely applied in literature since, in visual industrial applications, circular objects frequently occur both in natural and man-made scenes. A number of techniques have been applied in the last decade. The Hough transform (HT) and several modified versions have long been recognized as robust techniques for curve detection and have been largely applied by the scientific community [1–3].

The basic idea of the HT is to detect parameterized curves in images by mapping edge pixels into manifolds in the parameter space; methods to find peaks in the parameter space can be used to detect the image curves [4,5]. The main problem to be faced using the HT is the proper identification of peaks in the parameter space: false peaks in the image that are caused by a lot of spurious line and arc segments must be eliminated [6]. The heights of the desired peaks are not uniform, and the true peak is often surrounded by other peaks due to the presence of noise in the image. Furthermore, the computation of HT requires a large amount of memory storage space. Also, the choice of the quantization of the parameter space is a key point: if the size of the slot is small, it requires an enormous amount of storage space and produces sharp peaks (the peaks are distributed over neighboring slots); on the other hand, coarse quantization reduces the precision of parameters estimation. Besides it is not clear how fine the parameter space quantization should be in order to guarantee the convergence of the HT, i.e. that the true maximum is not missed. In [7] the conditions for the strict and wide sense convergence of the HT have been analyzed considering both random errors in locating edges and background noise.

Many researchers have been working to reduce the computational complexities, memory requirements, and the inaccuracy of Circle Hough Transform (CHT) in cases of very noisy images [8–12].

Several non-HT-based techniques for detecting circles have been also proposed [13–15]. In [14] geometric symmetry has been used to detect symmetric center location and parameter estimation both for ellipse and circle detection. A method based on the intersection of pairs of chords has been proposed in [15]. Least-squares techniques, centered on finding the set of parameters that minimize some distance measure between the data points and curve equations, have been also largely studied [16–19].

All the methods based on the search of a maximal value in an accumulation space always produce candidate peaks but give no guarantee that the selected one actually corresponds to a circle. The real experiments of the above methods have been carried out on industrial images, where circular patterns are well contrasted with respect to uniform backgrounds; in these cases the authors assert to have good results in detecting the circles parameters even with occlusion and noise.

We argue that the recognition process should require a robust method to validate the results of circle detection especially if the application context is complicated as the soccer game: a thresholding process cannot be applied to recognize circles as variable light conditions can modify the expected maximal values. In [20] a validation procedure based on 1D radius histogramming has been used to recognize circles and calculate their radius; among the experimental results the authors show that a circular soccer ball has been correctly recognized in a real image.

In contrast to these approaches are those based on learning by examples, where the recognition process is formulated as one of matching appearance rather than shape. Example-based approaches have been widely used in a number of applications such as face recognition, people detection, car detection and so on, where a geometric model of the searched pattern is not available or the object has complex geometric properties. In these applications a compact representation of the object appearance is needed to obtain a low-dimensional subspace taking into account varying pose and illumination. In [21–25] histogram equalization, wavelet-based preprocessing, parametric eigenspace decomposition have been applied to transform the image and then classify the resulting data vector.

In previous works [26,27] classification techniques based on support vector machine and neural network have been applied in the soccer context on both textured ball and non-textured ball. The detection rates are very high when the ball is completely visible in the image. Computational time is prohibitive for a real-time implementation. Indeed the classifiers are trained to recognize the ball using windows that are quite of the dimension of the ball (i.e. 20×20), then the process of classifying pattern is repeated at all locations in the image by shifting the window across and down the image. Also considering code optimization on specialized hardware the computation time remains far from making the recognition system applicable in real time.

The aim of our work is to develop an efficient ball recognition system that works well on real images with variable light conditions and non-controlled backgrounds, considering both computational aspects (the soccer context requires real-time processing) and system performances (false positive are not allowed if the goal event has to be detected).

The main contribution of this work consists of using together two different techniques in order to take advantages from the peculiarity of each of them: first of all, a fast circle detection (and/or circle portion detection) algorithm, based only on edge information, is applied on the whole image to limit the image area which is the best candidate to contain the ball; second, a neural classifier evaluates all the information contained inside the selected area to validate the ball hypothesis.

The circle detection algorithm is based on the circle Hough transform (CHT) that has been formulated as convolutions applied on the edge magnitude image [28]. The convolution kernels have been properly defined in order to detect the most completed circle in the image, being independent of the edge magnitude, and considering also different shapes of the ball according to different light conditions.

The sub-image containing the result of the detection process is forwarded to a neural network classifier trained to recognize "ball" and "no-ball" instances. In order to reduce the input data to the classifier, still maintaining the information properties that characterize the ball, different preprocessing have been applied to the selected area and the behaviors of the obtained classifiers have been compared on the same test images.

A large number of experiments has been carried out on real image sequences. Also varying light conditions have been considered in order to demonstrate the robustness of the ball recognition system.

The rest of the paper is organized as follows: Section 2 describes the system in detail. Section 3 reports the performance of our system on real image sequences. In Section 4 conclusions are presented.

2. System details

2.1. Overview of system architecture

Goal detection in soccer matches is an interesting application domain for pattern recognition techniques as a number of problems have to be solved. From a simple point of view, ball detection can be considered as the problem of detecting circular features in sequences of images when the light conditions produce the ball appearance in the image as a circular pattern. In fact, when using artificial lights (matches played in the evening) and shaded natural lights, the ball results very close to a spherical object in the scene. Unfortunately, in a directional and dominant sun light the ball appears in the image as a spherical cap whose orientation varies according to the sun orientation in the stadium: the detection and recognition techniques have to be tuned to detect different patterns the ball maps into the image due to the particular case we have to deal with.

Another very crucial aspect to face in this situation is the real time processing capacity of the system, if it should be used as a decision support to the referee committee. The ball can move at great speed during the game therefore an acquisition device with a very high frame rate should be used. The pattern recognition techniques, hence, have to be computationally efficient.

Our system operates in two stages (see Fig. 1): it first applies a circle (or circle portion) detection on the whole image to select the area that best fits the sought pattern. A neural classifier, working only on the selected area, then validates the decision on the identified pattern.

A fast circle detection operator based on the directional CHT has been implemented with simple convolutions; the a priori knowledge of the ball appearance (dimension of the ball, light conditions) have been used to set up the proper masks for the searched pattern. The main benefits of this approach are the low computational cost and the high detection rates when the ball is completely visible in the image. The main drawback lies in the impossibility of detecting occlusions and ball absence in the image. The circle detection

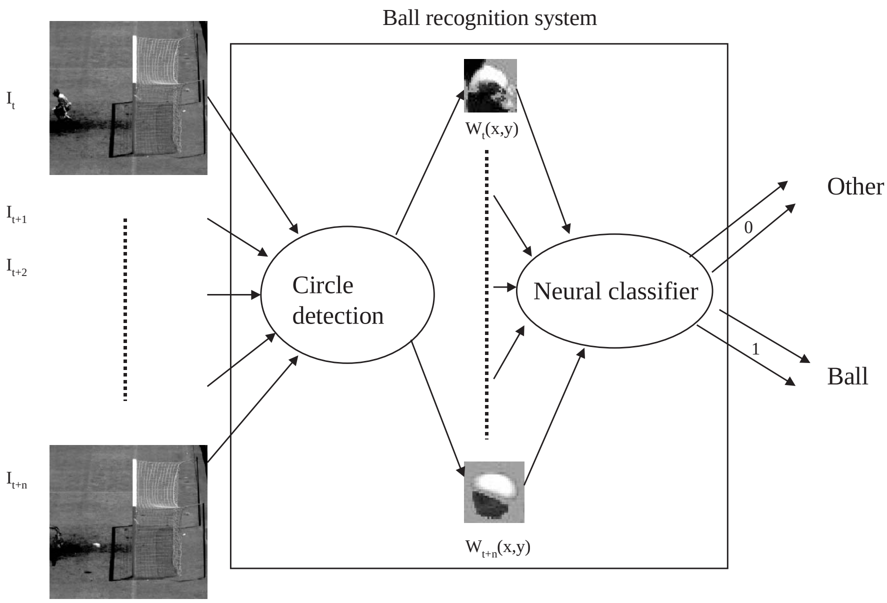

Fig. 1. System architecture: I_t is the image acquired at the time t; $W_t(x, y)$ is the sub-window candidate to contain the ball from the contour information.

Fig. 2. An image and the corresponding gradient module of a TV sequence.

algorithm determines in every situation the highest peak in the accumulator space. Then it is difficult to differentiate between images containing and not containing the ball.

A validation procedure is needed to decide if the pattern relative to the highest peak is correctly corresponding to the ball or not. To solve this problem the sub-image containing the result of the detection procedure has been used as input to a neural network trained to classify images as ball or no-ball instances. The classifier is applied only on the window that is candidate to contain the ball, avoiding the high-computational costs of the cited example-based techniques which scan the entire image [26,27].

2.2. Circle detection

The CHT aims to find circular patterns of a given radius R within an image. Each edge point contributes a circle of radius R to an output accumulator space. The peak in the output accumulator space is detected where these contributed circles overlap at the center of the original circle. In order to reduce the computational burden and the number of false positives typical of the CHT a number of modifications have been widely implemented in the last decade. The use of edge orientation information limits the possible positions of the center for each edge point. In this way only an arc needs to be plotted perpendicular to the edge orientation at a distance R from the edge point.

The CHT and also its modifications can be formulated as convolutions applied to an edge magnitude image (after a suitable edge detection) [28].

We have defined a circle detection operator that applied over all the image pixels produces a maximal value when a circle is detected with a radius in the range $[R_{\min}, R_{\max}]$

$$u(x,y) = \frac{\int\int_{D(x,y)} \vec{e}(\alpha,\beta)\cdot\vec{O}(\alpha-x,\beta-y)\,\mathrm{d}\alpha\,\mathrm{d}\beta}{2\pi(R_{\max}-R_{\min})}, \tag{1}$$

where the domain $D(x,y)$ is defined as

$$D(x,y) = \{(\alpha,\beta)\in\Re^2 \mid R^2_{\min} \leqslant (\alpha-x)^2+(\beta-y)^2 \leqslant R^2_{\max}\}, \tag{2}$$

$\vec{e}$ is the gradient versor

$$\vec{e}(x,y) = \left[\frac{E_x(x,y)}{|E|}, \frac{E_y(x,y)}{|E|}\right]^{\mathrm{T}} \tag{3}$$

and $\vec{O}$ is the kernel vector

$$\vec{O}(x,y) = \left[\frac{\cos(\tan^{-1}(y/x))}{\sqrt{x^2+y^2}}, \frac{\sin(\tan^{-1}(y/x))}{\sqrt{x^2+y^2}}\right]^{\mathrm{T}}. \tag{4}$$

The use of the gradient versor in (3) is necessary in order to have an operator whose results are independent of the intensity of the gradient in each point: we want to be sure that the circle detected in the image is the most complete in terms of contours and not the most contrasted in the image (see Fig. 2). Indeed it may happen that a circle not well contrasted in the image gives a convolution result lower than another object not exactly circular but with a greater gradient; in this case different results are obtained after the convolution with the original operator suggested by [28] and our scaled version. In Fig. 3 it is evident that our operator detects the peak correctly on the ball, while the not scaled version detects the peak on the "O" of the "SONY" advertising poster.

The kernel vector contains a normalization factor (the division by the distance of each point from the center of the kernel) that is fundamental in order to have the same values in the accumulation space when circles with different radius in the admissible range are found. Besides the normalization assures that the peak in the convolution result is obtained for the most complete circle and not for the greatest in the annulus.

As a last consideration, in Eq. (1) the division by $(2\pi(R_{\max}-R_{\min}))$ guarantees the final result of our operator in the range $[-1,1]$ regardless the radius value considered in the procedure.

The masks implementing the kernel vector are shown in Fig. 4. The dimension of these masks is $(2R_{\max}+1)\times(2R_{\max}+1)$ and essentially they represent in each point the direction of the radial vector scaled by the distance from the center. The convolution between the gradient versor images and these masks evaluates how many points in the image

Fig. 3. The peaks obtained with the Atherton operator and our modified operator.

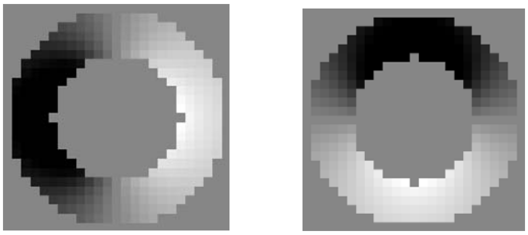

Fig. 4. The masks that implement the kernel vector $\vec{O}(x, y)$ in the domain $D(x, y)$.

have the gradient direction concordant with the gradient direction of a range of circles.

Then the peak in the accumulator array gives the candidate center of the circle in the image.

2.3. Circle detection with self-shadow

The $u(x, y)$ operator has good performance if the circle is well contrasted over the background, but unfortunately this is not a real situation when light produces self-shadowing effects on the circle. We have applied the program on soccer image sequences taken with natural light. The ball appears in every image as a white semicircle with a slope that depends on the direction of the sun (see Fig. 5).

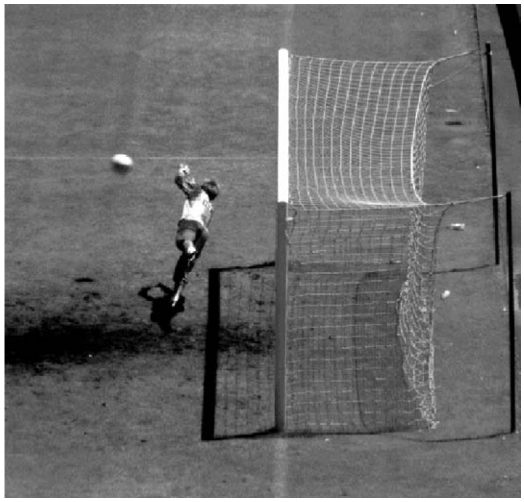

Fig. 5. An image acquired with natural light.

For this reason we have modified the $\vec{O}(x, y)$ operator in order to detect semicircles with different orientations.

$\vec{O}_\alpha(x, y)$ has been defined as follows:

$$\vec{O}_\alpha(x, y) = \begin{cases} \left[\dfrac{\cos(\tan^{-1}(\frac{y}{x}))}{\sqrt{x^2 + y^2}}, \dfrac{\sin(\tan^{-1}(\frac{y}{x}))}{\sqrt{x^2 + y^2}} \right]^{\mathrm{T}} \\ \quad \text{if } y \geqslant x(\tan(\alpha)), \\ [\cos(\alpha - 90^\circ), \sin(\alpha - 90^\circ)]^{\mathrm{T}} \\ \quad \text{if } |y - x(\tan(\alpha))| \leqslant \dfrac{R_{\max} - R_{\min}}{2}, \\ 0 \\ \quad \text{otherwise,} \end{cases} \tag{5}$$

where α is the slope of the semicircle diameter.

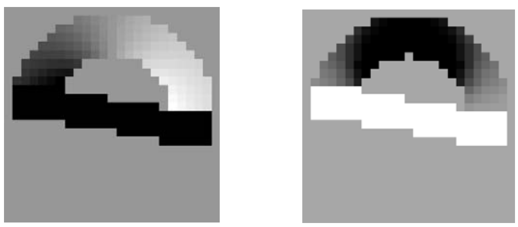

Fig. 6. The masks that implement the kernel vector $\vec{O}_\alpha(x, y)$ in the domain $D(x, y)$.

In Fig. 6 the new kernels for the detection of semicircles with diameter slope of -10° are shown.

The slope of the semicircle diameter can be dynamically modified as soon as the light conditions change in order to detect the ball during the whole match: since the geographical orientation of the soccer court and the camera positions are known, the variations of the sun position producing the self-shadow changes in the ball image can be forecasted and

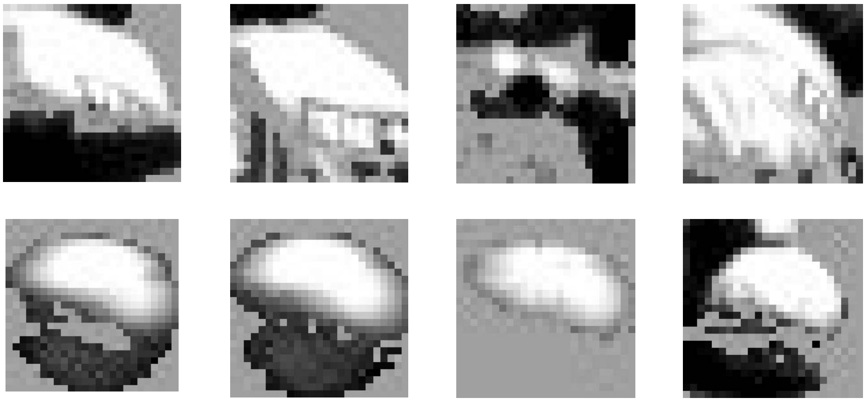

Fig. 7. Some images of a training set: in the first row there are some negative examples, in the second row some positive examples of the ball.

the detection masks can be chosen according to the assumed light conditions.

During preliminary tests we have compared the results obtained on the same sequences with the initial version of our algorithm and the modified one with the shadow information. There was a great increase of the performance. For this reason in the experimental phase for each image sequence we have applied the proper masks in order to obtain the maximum detection rate.

2.4. Neural classifier

The sub-image containing the result of the detection process is passed to a neural classifier trained to separate images as "ball" or "no-ball" instances. The neural network, trained with a back propagation algorithm, consists of three layers of nodes: the input layer has the number of nodes that depends on the number of coefficient selected after the image preprocessing (major details will be given in the rest of this section); the hidden layer has 80 nodes and the output layer has only one node. The neural network parameters have been found experimentally, choosing the combination that produces the best results in terms of ball detection rate. Examples of positive and negative sub-images given as input to the ball recognition process are shown in Fig. 7. In the second row of the figure there are some images of the ball after applying the background subtraction procedure. It comes out that the information of the ball concept is encapsulated both in texture and contour: there is a smooth region with little discontinuities and noise in the gray levels, which has a sharp separation with the background. It is necessary to understand if a more compact representation of the image can be used to store the main part of the image information in a small set of coefficients, still preserving the data characterizing the problem and taking into account the different appearances of the searched pattern with varying light conditions. Here the 2D Wavelet transform has been considered to convert the input image into wavelet coefficients at a lower resolution level.

2.4.1. The Wavelet representation

The Wavelet transform has been largely used in literature since it allows both to characterize the frequencies of the image and to localize them [29–34].

The Wavelet transform operator $F : L^2(R) \rightarrow L^2(R)$ can be defined as follows:

$$F(f(s)) = \hat{f}(s) = \int_{-\infty}^{\infty} f(u)\psi_{s,t}(u)\,\mathrm{d}u, \tag{6}$$

where

$$\psi_{s,t}(u) = \frac{1}{|s|^p}\,\psi\left(\frac{u-t}{s}\right) \tag{7}$$

varying s the frequencies on which the function ψ operates are changed, and varying t the function ψ is moved on all supports of the function f.

In this work a Discrete Wavelet transform has been used, supplying a hierarchical representation of the image implemented with the iterative application of two filters: a low-pass filter LPF (approximation) and its complementary in frequency HPF (detail filter). The mono-dimensional decomposition scheme is depicted in Fig. 8a.

At each step the Wavelet transform breaks the image into four sub-sampled images (sub-images), applying first on rows and then on columns the LP HP filtering scheme, followed by a decimator of factor 2. This procedure is iterated several times to obtain a full depth wavelet decompositions, re-applying the same scheme only on the low pass sub-image at each step. In Fig. 8b the sub-image arrangement scheme of a 3-level Wavelet transform is shown. The capital letters in each sub-image represent the kind of filters that have been applied on the image of the previous level; the first letter is the filter that has been applied in the horizontal direction, while the second letter is the filter that has been applied in the vertical direction (H stands for

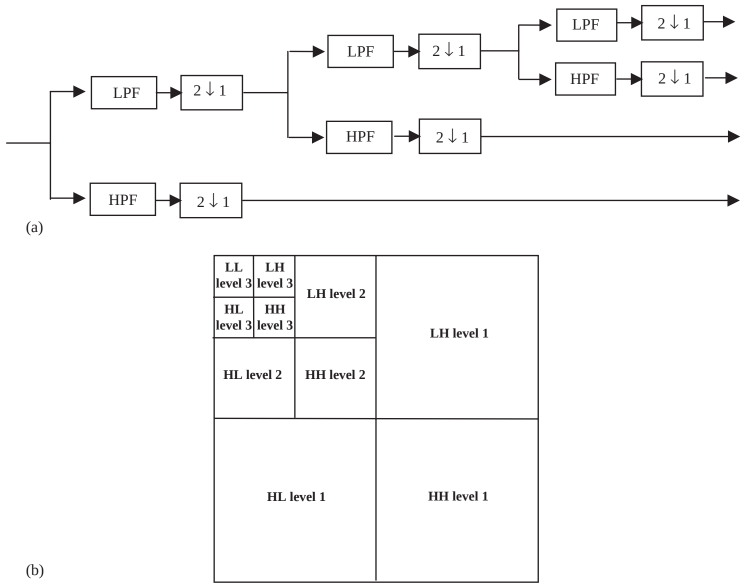

Fig. 8. The decomposition of the image with a 3-level Wavelet transform: (a) 1D decomposition scheme; (b) sub-image arrangement scheme.

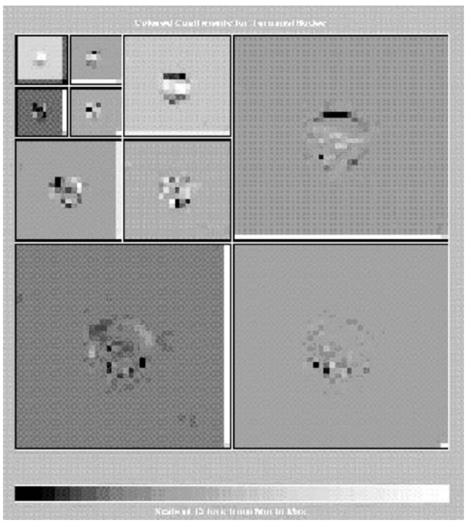

Fig. 9. The 3-level Wavelet transform on a sub-image containing the ball.

an high-pass filter L stands for a low-pass filter). The band LL is a coarser approximation of the original image. The bands LH and HL record the changes of the image along horizontal and vertical directions. The band HH shows the high-frequency components of the image. Decompositions can be iterated on the LL sub-bands. After applying a 3-level Wavelet transform, an image is decomposed into sub-bands of different frequency components. Fig. 9 shows the result of the application of a three stage wavelet decomposition on the ball image.

The coefficients of the wavelet transform enclose information about the texture and the shape of the object in the image. In this way it is possible to distinguish the ball from other elements that could have in common one of the two aspects. For example the head or the back of a player could have the same shape and size of the ball but it can be distinguished considering the texture information. In the first row of Fig. 7 there are some no-ball examples that have been erroneously detected in the first circle detection step. However a proper analysis of the texture information allows the classifier to distinguish them from the ball examples.

Different tests have been carried out in order to detect the best decomposition level, and the proper filter suitable for the problem at hand. Besides different dimensions of the images have been considered in order to have the highest detection rate of the neural classifier. The results are shown in Section 3.2.

3. Results

The tests have been carried out on different sequences of images taken during training matches both with artificial and natural light conditions. The camera has been placed on a side of the soccer field with its optical axis lying on the goal-mouth plane. The background subtraction has been applied producing sequences of images, where only the moving structures are highlighted. In this way the circle detection algorithm does not produce false detection on fixed circular structures of the environment (such as advertising poster), but it can give false positive detection only on moving players.

Table 1
The performances of AA and MAA on images with artificial light condition

SEQ	Number of images	AA detected circle	MAA detected circle
1	158	135	141
2	78	43	71
3	150	131	150
4	203	47	181
Image Tot.	589	356	543
Detection rate		60%	92%

Table 2
The performances of AA* and MAA* on images with natural light condition using masks of Fig. 6

SEQ	Number of images	AA* detected circle	MAA* detected circle
5	100	13	90
6	58	55	55
7	75	17	74
8	164	164	164
9	30	30	30
10	66	65	65
11	30	30	30
12	61	61	61
Image Tot.	584	435	569
Detection rate		74%	97%

The experimental phase has been divided in two parts: in the first one the ball detection algorithm has been evaluated on the sequences acquired both with artificial and natural light conditions; in the second part different preprocessing (different choices of the decomposition level, different kinds of filters and different dimensions of the window) have been applied on sequences acquired with natural light condition in order to establish the solution that gives the best performance of the ball recognition algorithm.

3.1. Ball detection experimental results

Our algorithm has been compared with the one suggested by [28]. For the sake of completeness we have tested also the original CHT on the same image sequences. The implementation of the CHT by convolution with a binary mask has been applied on binary images of the edges obtained by the Canny algorithm. A number of trials were necessary to detect the proper thresholds tuned on each sequence. For this reason in the following experiments we have considered only the circle detection routine based on the edge orientation as no edge thresholding is required.

The image partial derivatives have been estimated by convolving the image with the derivatives of the Gaussian kernel.

In the following the Atherton algorithm will be referred with AA, while our proposed algorithm will be denoted with MAA (modified Atherton algorithm). Twelve sequences have been considered in the testing phase: four sequences have been taken with artificial light and the ball appears as a complete circular shape; eight sequences have been taken with natural light so that the ball, due to the self shadow effect, appears as a semicircle in every image.

The results obtained on the four sequences with artificial light using the masks of Fig. 4 are shown in Table 1. The results obtained on sequences with natural light using the masks of Fig. 6 are shown in Table 2. The MAA algorithm gives always an higher detection rate because the most completed balls in terms of contour directions are easily found. The AA algorithm fails on a greater number of images as the intensity of the gradient produces maximum values on more contrasted parts of the image such as the jersey of the players. The sequences where the differences in the performances are larger, are indeed the ones where the player wears a white shirt that results more contrasted compared to the ball.

In the following part of the experiments the results obtained with the MAA algorithm have been considered as input to the ball recognition process.

3.2. Ball recognition experimental results

The output of the previous detection step is the position of the area in the images candidate to contain the ball. The validation procedure must determine if the ball is present in this area or a false positive has been detected. The image portion around the position of this area can be selected by a window and considered as input to the validation procedure. The training set contains 341 positive examples and 593 negative examples.

As the results of the whole ball recognition system depend on the proper definition of several parameters, in this section comparisons of several choices will be reported together with the resulting performances.

In particular the main interests are focused on the definition of the convenient size for the analysis window to be used, the preprocessing procedures necessary to improve the classification performance and finally the effects of varying light conditions and reducing the number of coefficients.

3.2.1. Detection of the window size

For the application domain considered the first problem concerns the proper determination of the size of the window around the position provided by the detection step. Different factors should be considered in order to decide this size.

From the analysis of the sequences acquired during real matches with the camera in a fixed position and with a fixed focal length, we observed that the ball radius was around 12 pixels. Therefore, the minimum size for the window to

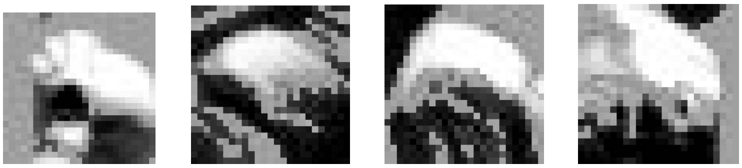

Fig. 10. Examples of selected windows: difficult classifications even for humans.

contain the whole ball can be 25×25 pixels. If this minimum size 25×25 is considered it should be clear that some edge information can be lost (the positions where the ball is tangent to the window) and meanwhile all the information of the background, that can be useful for the classification, is eliminated. This last consideration is very important to evaluate the results of the classifier: indeed often the human recognition of an object from similar elements is greatly helped by the background information because the discrimination based only on the selected pattern can be very difficult.

The Fig. 10 shows some examples in the soccer images where the classification can be very hard if a small window is considered. In these cases it is difficult also for humans to establish if this pattern corresponds to an occluded ball or it is a different object.

This problem can be overcome taking a larger window, for example 75 by 75 pixels, enclosing both the pattern and the background information. It is important to remember that the background includes only moving objects, since static objects are eliminated by the background subtraction procedure. With larger window human recognition is greatly improved as the background information detains a huge quantity of details that help the discrimination from similar objects.

Unfortunately, this is not the same for a neural classifier: there are infinite positions of the ball and possible background objects. Therefore, training the classifier is very difficult and can never be complete. The recognition of the ball can be guaranteed only when the ball is far from other moving objects (i.e. the background in the window is very clear). In other cases the classifier cannot recognize the ball even if it is present in the window together with other objects. In [35,36] the experiments have been carried out using these larger windows. In those cases the main objective was to detect the first image of the sequence containing the ball in order to activate a tracking procedure. For that problem the recognition algorithm must guarantee a very low percentage of false positive, to be sure of tracking the ball and not a different object. In this paper the main objective is the recognition of the ball in each image of the sequence, then not only a low percentage of false positive but also a low percentage of false negative should be achieved; smaller windows give the best guarantees for the correct classification of both ball and no-ball images.

Another consideration concerns the choice of the preprocessing procedure. The kind of preprocessing will be discussed later in this section. However, in some way it will affect also the window dimension. If wavelet decomposition is used, particular care should be made in selecting the image portion to be processed. As the image of the ball is a very smooth surface in the acquired video sequence, the maximum portion of information is concentrated around low frequency, while high-frequency terms of the image decomposition contain mainly the ball edge information and noise. The edges of the ball should all appear undistorted in the wavelet decomposition, so that the window has to be larger than the 25×25 pixel size assumed. A certain guard ring in the window to be used in the image analysis has to be taken into account. Longer filters improve frequency selectivity, but the longer is the used analysis filter's impulse responses, the larger has to be the guard ring of the window to be used. Also in this case introducing a guard ring can be the source for unwanted uncertainty in the validation process, as other moving objects (different from the ball) can appear in the analysis window. The presence of other objects in the window affects the wavelet coefficient computation and thus image validation performance. Although the use of longer filters can improve the frequency selectivity of the image description, the unwanted presence of other objects distorts wavelet coefficients so a proper trade-off has to be searched to maximize the validation procedure performances.

Simulations have proved that even if long impulse response filters show higher frequency discrimination properties, they require larger windows so that the validation process fails more frequently than in the case of using short filters (i.e. a smaller guard ring), due to the discussed possible presence inside it of other moving objects.

In particular, if Haar wavelet is applied, due to its very short impulse response filter (two samples), the smallest window size also performs properly and allows in most cases undistorted wavelet coefficients computation. This couples well to the requirement of efficiency of the algorithm: the computation complexity of the wavelet decomposition grows quadratically with the filter length.

This last consideration is in some way connected to the last point analyzed. The computational times both for the training and the tests can be very long if the number of coefficients provided to the classifier is large. In this case some reduction is required to decrease the input to the classifier.

The discussed points brought us to the conclusion that window size of 25 by 25 pixels is the best choice for our domain.

(a) (b) (c)

Fig. 11. Three frames of the sequences: (a) ball completely visible, (b) ball partially occluded, (c) ball completely occluded.

Table 3
The classifier performance without preprocessing

Correct classification of "ball" (%)	Correct classification of "no-ball" (%)	Correct classification of "occluded ball" (%)	Correct classification percentage (%)
99.37	97.80	86.33	96.46

3.2.2. Preprocessing procedure

The second problem concerns the decision of the kind of information that should be provided to the classifier in order to obtain the best performance. All the pixels in the window can be directly supplied to the classifier in their original form. Of course, no-preprocessing is the favorite solution if the main requirement for the whole system is efficiency. This is the first and easiest method for training the classifier. Anyway, if varying light conditions have to be considered, features better characterizing the object in the window are necessary. As it will be clear in the next sub-section, the use of gray levels for the classifier would claim for continuous re-training (or updating of pre-trained sequences in different light conditions) and this is impossible during the match. This problem can be overcome by using a new representation of the object based on its specific frequency and time peculiar characteristics: the wavelet representation.

The approximation coefficients (low pass terms) supply information on gray levels in the image but the detail coefficients supply information on variations in neighboring pixels and are independent of the value of the single pixel. For this reason the information of the detail coefficients (high-frequencies terms) allow to classify correctly the ball also in varying light conditions, without any need of a new training phase for the classifier.

The Wavelet transform can also provide an easy instrument to reduce the coefficients considering a decomposition of the image with multi-resolution levels.

A number of experiments have been carried out to compare the classification performances with different preprocessing procedures against no preprocessing at all. The classification is based on a back propagation neural network as described in Section 2.4.

Several wavelet preprocessing procedures have been tested considering different implementation choices such as the wavelet family and the level of decomposition.

The tests have been performed on a complex sequence of 821 images. The complexity of the sequence derives from the presence of two players (the goal keeper and the forward) in an action with multiple shots on goal. The following table resumes the ball situations in the test sequence:

Target	Number of images
Ball	318
No-ball	364
Occluded ball	139

This classification has been done as follows: the ball has been considered completely visible even if a small percentage of its surface is occluded (less than the 25%); it has been considered occluded if a percentage of its surface varying between 25% and 50% is not visible for the presence of shadows, players or goal-post; no-ball cases include both images where the ball is absent and images where the ball is occluded for more than the 50% of its area. In the last cases also human recognition of the ball can be difficult due to the lack of information. In Fig. 11 three frames of the test sequence are shown.

Table 3 resumes the classification results without preprocessing supplying to the neural network directly the gray

Table 4
The classifier performance with Wavelet preprocessing

Wavelet family	Decomposition level	Correct classification of "ball" (%)	Correct classification of "no-ball" (%)	Correct classification of "occluded ball" (%)	Correct classification percentage (%)
Haar	1	99.37	98.62	84.89	96.58
Haar	2	99.05	98.07	85.61	96.34
Haar	3	98.74	98.90	87.05	96.83
Haar	4	98.42	99.17	92.08	97.68
Daub. 2	3	98.74	98.35	89.20	96.95
Daub. 3	3	97.79	99.17	89.20	96.95
Daub. 3	4	98.42	98.07	82.73	95.61
Daub. 4	3	98.11	98.62	91.36	97.19
Daub. 4	4	99.05	98.35	77.69	95.12

levels of the window. In this case there are $25 \times 25 = 625$ input elements. The classification rates for the three types of images of the test sequence have been reported together with the overall classification percentage evaluated considering the number of images in each set.

The preprocessing procedures have been applied considering different families of wavelet filters as Haar, Daubechies 2, Daubechies 3, Daubechies 4 with different decomposition levels. All the 625 coefficients have been provided as input to the neural classifier. Table 4 resumes the experimental results. The best classification percentage has been obtained with the family of Haar filters at the fourth level of decomposition that supplies the best space-frequency representation of the original image for ball classification. This result agrees with the hypothesis about the filter choice made in the previous subsection. Since the goal of this work is to develop a ball recognition system for detecting critical events, to estimate the effectiveness of the system the most important parameter is the percentage of the correct classification of no-ball. During a soccer match it would be really unpleasant to have false alarms of goal detected whenever a pattern similar to the ball (such as the shoulder or the shorts of a player) is accidentally found behind the door-post. The detection rate of no-ball images above the 99%, is a good guarantee of avoiding these false alarms. Anyway the recognition is assured when the ball is completely visible since the correct detection rate is over the 98%. Lower detection percentages have been obtained with all the families of filters when the ball is occluded. However, false negatives of occluded ball can be easily recovered with few efforts considering a ball tracking procedure in the sequence.

The last consideration concerns the comparison of the wavelet preprocessing with no-preprocessing. Tables 3 and 4, show that the performance are not so far: no-preprocessing gives an overall classification percentage of 96.46% while the Haar filter with the fourth decomposition level gives 97.68%. If only these results were compared the choice of no preprocessing would be the best solution also considering that the wavelet decomposition takes some computational time. But varying light conditions should be taken into account: the classifier performances are less sensitive to varying light condition if the wavelet coefficients are provided as input. This argument will be the subject of the next subsection.

3.2.3. Variations of light conditions

All the experiments presented in the Section 3.2 have been produced on real images taken during a soccer match with sunned light conditions. The analysis of all the sequences shows that there is not a great variation of the light among the test and the training images. However, during the 90 min. of the match some variations of the intensity values might happen. For this reason we have artificially modified the test images to evaluate the robustness of the classifier and compare the results obtained with no-preprocessing and the wavelet transform with the Haar filters.

Variations of the light conditions are simulated with the formula below:

$$I'(x, y) = \alpha I(x, y) - K, \tag{8}$$

where α is a parameter larger than 1 and K is given by

$$K = m' - m$$

with

$$m = \frac{\sum_{x=1}^{\dim x} \sum_{y=1}^{\dim y} I(x, y)}{\dim x \dim y} \quad \text{and}$$

$$m' = \frac{\sum_{x=1}^{\dim x} \sum_{y=1}^{\dim y} I'(x, y)}{\dim x \dim y}.$$

Fig. 12 shows the results of this method on one of the test images. Table 5 resumes the classification results without preprocessing by using two different values of the parameter α.

Table 6 shows the results obtained with the wavelet preprocessing by using the Haar filter at the fourth decomposition level.

As expected the classifier performances decrease when α increases, but the preprocessing technique guarantees a minor sensitivity to these variations. The performance of

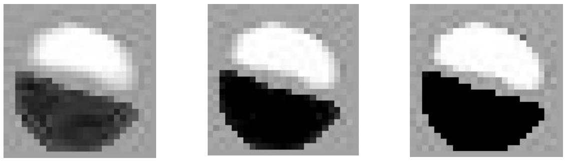

(a) (b) (c)

Fig. 12. (a) Original image, (b) variation with $\alpha = 1.5$, (c) variation with $\alpha = 2$.

the classifier with $\alpha = 2$ remains over 97% with the best family of the filtering techniques. Without preprocessing, when α varies, all the gray levels change and thus the neural network has major problems to classify correctly the test samples because the coefficients learned in the training phase are different. On the contrary by using preprocessing, only the approximation coefficients in the wavelet decomposition change while the detail coefficients remain invariant. The central idea is that the approximation coefficients, that supply information on gray levels, are very few with respect to the detail coefficients, that supply information on variations in neighboring pixels and are independent from the value of single pixel.

3.2.4. Normalization

The purpose of this paragraph is to evaluate the use of a normalization step to take care of the light conditions changes.

The normalization has been defined here by

$$I(x,y) = \frac{I(x,y) - I_o(x,y)}{\sigma(x,y)}, \tag{9}$$

where

$$\sigma(x,y) = \sqrt{\frac{1}{D(x,y)} \sum_{(n,m)\in D(x,y)} (I(x-n,y-m) - I_o)^2},$$

$$I_o(x,y) = \frac{1}{D(x,y)} \sum_{(n,m)\in D(x,y)} I(x-n,y-m). \tag{10}$$

In (9), $I(x,y)$ is the patch to be used in the classification step, $I_o(x,y)$ is the average gray level value computed over the neighborhood $D(x,y)$ of the (x,y) point in the given patch, and $\sigma(x,y)$ is the local standard deviation of the patch, computed in the same neighborhood $D(x,y)$.

Tests have been conducted with different neighborhood extension $\mathrm{D}(x,y)$; the best performance of the normalization scheme has been obtained when $D(x,y)$ covers all the patch. In this case, the standard deviation is simply a scaling coefficient, and the resulting image shows a zero mean and unitary std deviation.

The model illumination change is thus simply transformed by means of a linear function in order to always have the same dynamic range of the given patch.

The neural network has been retrained with normalized patches. Also, each candidate to the classification step has been first normalized and then classified. Results of this classification step are reported in subsequent tables in quantitative form.

Tests have been conducted on both "ball" and "no-ball" cases considering constant and changing light conditions; results compare the performances obtained with the proposed approach with and without the normalization preprocessing.

Table 8 shows results of the ball classification rate without light condition changes, while in Table 7 two different light variation coefficients have been used to simulate light conditions changes as described in (8) and the results have been compared with and without the normalization preprocessing.

It is noteworthy from Tables 7 and 8 that the correct classification of "no-ball" and "occluded ball" rapidly decrease for the proposed normalization preprocessing, particularly in presence of light conditions changes.

This result can be justified considering that the normalization phase shifts the class of "no-ball" examples closer to the class of "ball" examples, rising the rate of wrong decisions.

In Fig. 13 two images of "ball" and "no-ball" before and after normalization are shown. The recognition system properly classifies the two images without the normalization step;

Table 5
The classifier performance without preprocessing, varying the light conditions

α value	Correct classification of "ball" (%)	Correct classification of "no-ball" (%)	Correct classification of "occluded ball" (%)	Correct classification percentage (%)
1.5	98.74	95.05	78.41	93.66
2	96.54	94.78	73.38	91.83

Table 6
The classifier performance with Wavelet preprocessing (Haar filters at the fourth decomposition level), varying the light conditions

α value	Correct classification of "ball" (%)	Correct classification of "no-ball" (%)	Correct classification of "occluded ball" (%)	Correct classification percentage (%)
1.5	98.74	97.25	96.40	97.68
2	99.05	95.60	97.12	97.19

Table 7
The classifier performance with and without the normalization processing in the case of simulated light conditions change

Light variation coeff.	Preprocessing	Correct classification of "ball" (%)	Correct classification of "no-ball" (%)	Correct classification of "occluded ball" (%)	Correct classification percentage (%)
1, 5	With normalization	99.37	86.81	86.33	91.59
	Without normalization	98.74	97.25	96.40	97.68
2	With normalization	98.37	78.84	89.92	88.67
	Without normalization	99.05	95.60	97.12	97.19

Table 8
The classifier performance with and without the normalization processing in the case of no light conditions change

Preprocessing approach	Correct classification of "ball" (%)	Correct classification of "no-ball" (%)	Correct classification of "occluded ball" (%)	Correct classification percentage (%)
With normalization	99.37	90.93	87.05	93.54
Without normalization	98.42	99.17	92.08	97.68

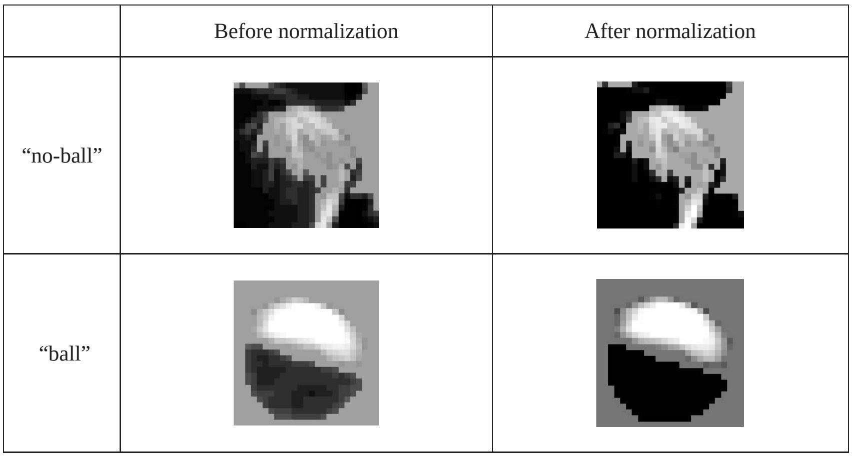

Fig. 13. Comparison between "ball" and "no-ball" cases before and after the normalization step.

in case of normalization preprocessing the "no-ball" image has been wrongly classified as "ball". Indeed, the normalization step has stretched the gray level values on the same range of the ball case; the clearest pixels of the "no-ball" image are more similar to the corresponding points of one of the "ball" examples. The same consideration can be done for the other images of "no-ball" and "occluded ball" on which wrong decisions have been taken.

Concluding the use of a normalization preprocessing procedure does not improve the performance of the recognition system; even if the correct classification rate of "ball" cases seems in same way to improve, the general behavior of the recognition system worsens especially in the more strategic cases of "no-ball" images. Simple wavelet preprocessing remains the best way to take care of possible light conditions change for our application domain.

3.2.5. *Coefficients reduction*

The last point considered in the experimental phase is the possibility to reduce the number of coefficients provided to the classifier in order to decrease the computational costs. Although the wavelet preprocessing can burden the computational load, it offers the possibility to consider different levels of representation. For this reason another experiment has been done: subsets of Haar wavelet coefficients at different decomposition levels have been extracted and the performances compared with that obtained providing all the coefficients to the classifier. Table 9 resumes the experimental results: it can be observed that decreasing the number of coefficients also the overall classification rates decrease. If only the coefficients of the third and fourth level of decomposition are considered (36 in total) the classifier reaches the detection of about 93%.

Table 9
The classifier performance with Haar filters and different numbers of coefficients

Coefficients selected	Number of coefficients	Correct classification of "ball" (%)	Correct classification of "no-ball" (%)	Correct classification of "occluded ball" (%)	Correct classification percentage (%)
Levels: 3,4	36	93.39	98.35	82.73	93.78
Levels: 2,3,4	144	95.59	98.62	87.05	95.49
Levels: 1,2,3,4	625	98.42	98.62	92.08	97.68

The decision of reducing the coefficients has to be done considering the proper trade-off between the performance that should be achieved and the processing time for real time implementations.

The software has been implemented by using Visual C ++ on a Pentium III 1 Ghz without any image processing specialized hardware. Although not all the code optimizations have been completed the actual processing time seems encouraging for a real time implementation. The processing of a 532×512 image takes less than 3×10^{-1} s, whereas the processing of a sub-image takes 4×10^{-3} s when a tracking procedure of the ball is activated. The introduction of code optimizations and the use of specialized hardware for the convolution procedures will produce real time performances in order to allow real experimentation during soccer matches.

4. Conclusions

In this work, an efficient ball recognition system that works on real images with variable light conditions and non-controlled backgrounds has been implemented. The choice of the method has been done mainly considering computational aspects (the soccer context requires real time processing) and system performances (false positive are not allowed if the goal event has to be detected).

The novelty of this work consists of using together two different techniques in order to take advantages of the peculiarity of each of them: a fast circle detection (and/or circle portion detection) algorithm is applied on the whole image to have the area that is the best candidate to contain the ball considering only the edge information; a neural classifier is used on the selected area to validate the ball hypothesis evaluating all the information contained inside the area.

The circle detection algorithm is based on the CHT that has been formulated as convolutions applied on the edge magnitude image. The convolution kernels have been properly defined in order to detect the most completed circle in the image, being independent on the edge magnitude, and considering also different shapes of the ball according to different light conditions.

The sub-image containing the result of the detection process is forwarded to a neural network classifier trained to recognize "ball" and "no-ball" instances. Different preprocessing techniques have been applied to the selected area and the behaviors of the classifier have been compared on the same test images in order to understand the best way to represent the information contained in our pattern. Also variations of light conditions have been considered in order to demonstrate the robustness of the ball recognition system.

A large number of experiments have been carried out on real image sequences. The Haar family at the fourth decomposition level produces the best performance. Also with variations of gray levels the Haar family maintains high performances. The main result of this work is that the number of false positive when the ball is completely visible, and the number of false negative, is very few. The percentages of correct detection are lower when the ball is occluded (still remaining over the 92%), but this situation can be easily recovered by introducing a ball tracking procedure in the sequence. The last point is outside the scope of this work, since our main objective was to establish the performance of the ball detection system leaving out of consideration the possible introduction of heuristics such as motion prediction, reduction of the search area and so on.

The results are very encouraging for building an automatic ball recognition system that can support the team of referees to take a decision when doubtful situations happen during a match.

Acknowledgements

The authors thank the anonymous referees whose valuable suggestions helped to improve the quality of the experimental results section.

References

[1] J. Illingworth, J. Kittler, A survey of the Hough transform, Comput. Vision Graph. Image Process. 44 (1988) 87–116.
[2] V.F. Leavers, Survey: which Hough transform, Image Understanding 58 (1993) 250–264.
[3] A. Sewisy, F. Leberl, Detection ellipses by finding lines of symmetry in the images via an Hough transform applied to straight lines, Image Vision Comput. 19 (2001) 857–866.
[4] R.O. Duda, P.E. Hart, Use of the Hough transformation to detect lines and curves in picture, Commun. ACM 15 (1972) 11–15.

[5] E.R. Davies, A modified Hough scheme for general circle detection, Pattern Recognition Lett. 7 (1988) 37–43.

[6] P. Kierkegaard, A method for detection of circular arcs based on the Hough transform, Machine Vision Appl. 5 (1992) 249–263.

[7] M. Soffer, N. Kiryati, Guaranteed convergence of the Hough transform, Comput. Vision Image Understanding 69 (2) (1998) 119–134.

[8] J.K. Goulermas, P. Liatsis, Genetically fine-tuning the Hough transform feature space for the detection of circular object, Image Vision Comput. 16 (9/10) (1998) 615–625.

[9] C.F. Olson, Constrained Hough transform for curve detection, Comput. Vision Image Understanding 73 (3) (1999) 329–345.

[10] N. Bennet, R. Burridge, N. Saito, A method to detect and characterize ellipses using the Hough transform, IEEE Trans. Pattern Anal. Mach. Intell. 21 (7) (1999) 652–657.

[11] H. Kalviainen, P. Hirvonen, L. Xu, E. Oja, Probabilistic and non-probabilistic Hough transform: overview and comparisons, Image Vision Comput. 13 (4) (1995) 239–252.

[12] O. Chutatape, L. Guo, A modified Hough transform for line detection and its performance, Pattern Recognition 32 (1999) 181–192.

[13] T.C. Chen, K.K. Chung, An efficient randomized algorithm for detecting circles, Comput. Vision Image Understanding 83 (2) (2001) 172–191.

[14] C. Ho, L.H. Chen, A fast ellipse/circle detector using geometry symmetry, Pattern Recognition 28 (1) (1995) 117–124.

[15] H.S. Kim, J.H. Kim, A two-step circle detection algorithm from the intersecting chords, Pattern Recognition Lett. 22 (6/7) (2001) 787–798.

[16] W. Gander, G.H. Golub, R. Strebel, Least-square fitting of circles and ellipses, BIT 43 (1994) 558–578.

[17] G. Taubin, Estimation of planar curves, surfaces and non-planar space curves defined by implicit equations, with applications to edge and range image segmentation, IEEE Trans. Pattern Anal. Machine Intell. 13 (11) (1991) 1115–1138.

[18] P.L. Rosin, G.A. West, Non-parametric segmentation of curves into various representations, IEEE Trans. Pattern Anal. Machine Intell. 17 (12) (1995) 1140–1153.

[19] Z. Wu, L. Wu, A. Wu, The robust algorithms for finding the center of an arc, Comput. Vision Image Understanding 62 (3) (1995) 269–278.

[20] D. Ioannou, W. Huda, A. Laine, Circle recognition through a 2D Hough transform and radius histogramming, Image Vision Comput. 17 (1999) 15–26.

[21] H. Murase, Visual learning and recognition of 3D objects from appearance, Int. J. Comput. Vision 14 (1995) 5–24.

[22] C. Papageorgiou, M. Oren, T. Poggio, A general framework for object detection, Proceedings of International Conference for Computer Vision, January 1998.

[23] H. Rowley, S. Baluja, T. Kanade, Neural network-based face detection, IEEE Trans. Pattern Anal. Machine Intell. 20 (1) (1998) 23–38.

[24] M. Jones, T. Poggio, Mode-based matching by linear combinations of prototypes, Proceedings of Image Understanding Workshop, New Orleans, LA, May 1997.

[25] A. Mohan, C. Papageorgoiu, T. Poggio, Example-based object detection in images by components, IEEE Trans. Pattern Anal. Mach. Intell. 23 (4) (2001) 349–361.

[26] N. Ancona, G. Cicirelli, A. Branca, A. Distante, Ball recognition in images for detecting goal in football, ANNIE 2001, St. Louis, MO, November 2001.

[27] N. Ancona, G. Cicirelli, A. Branca, A. Distante, Goal detection in football by using support vector machine for classification, International Joint INNS–IEEE Conference on Neural Network, Washington, DC, July 2001.

[28] T.J. Atherton, D.J. Kerbyson, Size invariant circle detection, Image Vision Comput. 17 (11) (1999) 795–803.

[29] S. Mallat, A Wavelet Tour of Signal Processing, Academic Press, New York, 1999.

[30] A.N. Akasu, R.A. Haddad, Multiresolution Signal Decomposition: Transforms, Subbands, and Wavelets, Academic Press, London, 1992.

[31] A.N. Akasu, M.J.T. Smith, Subband and Wavelet Transforms, Academic Press, Boston, 1996.

[32] A. Aldroubi, E. Lin (Eds.), Wavelets, Multiwavelets, and their applications, Contemporary Mathematics, AMS, Providence, 1998.

[33] L. Cohen, Time-frequency Analysis, Prentice Hall, Englewood Cliffs, NJ, 1995.

[34] R. Coifman, Y. Zeevi (Eds.), Signal Image Representation in Combined Space, Academic Press, London, 1997.

[35] T. D'Orazio, M. Leo, M. Nitti, A. Distante, Ball recognition in real sequence of soccer images with different light conditions, Proceeding of IEEE Conference on Systems, Cybernetics and Informatics, Orlando, July 2002.

[36] T. D'Orazio, M. Leo, M. Nitti, G. Cicirelli, A real time ball recognition system for sequences of soccer images, Proceeding of IASTED SPPRA Conference, Crete, Greece, June 2002.

About the Author—TIZIANA D'ORAZIO received the degree in Computer Science from the University of Bari (Italy) in 1988. Since 1989 she has worked at the Institute of Signal and Image Processing of the Italian National Research Council (CNR). She is currently a researcher of the Institute of Intelligent Systems for Automation of the CNR. Her research interests include pattern recognition, artificial intelligence, image processing for robotic application and intelligent systems.

About the Author—CATALDO GUARAGNELLA was born in Italy in 1964. He graduated in Electronic Engineering in 1990 from the University of Bari, Italy, and received the Ph.D. degree in Telecommunications from the Politecnico di Bari in 1994. In 1996 he joined the Electrics and Electronics Department of Politecnico di Bari as assistant professor in Telecommunications. His main research interests include signal and image and video processing/coding, motion estimation in video sequences and multidimensional signal processing.

About the Author—MARCO LEO was born in Gallipoli, Lecce, Italy in 1974. He received the degree in Computer Science Engineering from the University of Lecce in 2001. Since then, he is a collaborator of research at the Italian National Research Council (CNR), Institute of Study of Intelligent Systems for Automation (ISSIA) in Bari, Italy. His research interests are in the area of image and signal processing, neural networks and pattern recognition.

About the Author—ARCANGELO DISTANTE received the degree in Computer Science from the University of Bari (Italy) in 1976. He joined the National Nuclear Physics Institute until 1983 where he worked on various theoretical and computation aspects of 3D reconstruction and pattern recognition of nuclear events. Since 1984 he has been working with the Institute for Signal and Image Processing (IESI) of Italian National Research Council (CNR). Currently he is the coordinator of the Robot Vision Group and the Director of the Institute of Intelligent System for Automation (ISSIA—CNR). In 1996 he joined the University of Lecce where he is associate professor in Theory and Practice of Image Processing at the Faculty of Engineering. His current research deals with computer vision, pattern recognition, machine learning, neural computation, robot navigation and architectures for computer vision. Dr. Arcangelo Distante is a member of IAPR and SPIE.